Journal of Petroleum Exploration and Production Technology (2019) 9:1089–1104
https://doi.org/10.1007/s13202-018-0524-6

ORIGINAL PAPER - PRODUCTION ENGINEERING

Experimental investigation of hydrate formation, plugging and flow properties using a high-pressure viscometer with helical impeller

Ben Bbosa[1] · Evren Ozbayoglu[1] · Michael Volk[1]

Received: 23 May 2018 / Accepted: 21 July 2018 / Published online: 28 July 2018

Abstract

Slurry transport has become a subject of interest in several industries, including oil and gas. The importance of slurry/solid transport in the oil and gas industry is evident in areas of cuttings transport, sand transport and, lately, hydrates. Hydrate formation, if not properly monitored and controlled, may lead to pipeline blockage. To avoid pipeline blockage and other hydrate formation risks, chemical additives are added to the system. Additives such as anti-agglomerants help improve hydrate transportability by dispersing the formed hydrates into slurries and preventing them from sticking to the pipe wall. This enables transportation of highly concentrated slurries. However, the high hydrate volume fractions (HVF) slurries may exhibit complex rheology. There is therefore a great need to correlate flow properties such as friction factor and viscosity to HVF. Hydrate slurry transport is important whether hydrates are deliberately generated for energy storage purposes or hydrates formed because of the prevailing flow conditions. However, when determining the viscosity of a fluid containing solid particles, the conventional viscometer types such as concentric cylinders and cone and plate are often not suitable. This is because either the narrow gap would not accommodate the particle size or their inability to maintain the particles suspended leading to bed formation. In this work, a high-pressure mixer-type viscometer was used to generate and characterize hydrate slurries. This work aims to generate a significant amount of hydrate slurry characterization data that may be used as basis for better rheometer designs, hydrate slurry flow properties modeling or integration of hydrate transportability into general multiphase modeling. Results showed that intermediate watercuts posed the greatest pipeline plugging risk for all the oils tested. The amount of transportable hydrates increased with oil viscosity. Generally, hydrate slurries generated exhibited shear thinning behavior that increased with increasing hydrate volume fraction. However, the overall rheology of these slurries is a complex function of the oil used, watercut, gas added to the system and hydrate solid fraction. Lowering shear rates for high HVF systems resulted in separation. Results in this work further suggest that hydrate transportation may be possible with minimum risk if anti-agglomerants are used and high enough shear is applied. On the other hand, if no anti-agglomerant is used, severe aggregation may result in flow line plugging.

Keywords Hydrate slurry · Flow line plugging · Slurry transport · Slurry characterization · Complex rheology

Introduction

Hydrate formation observation dates as far back as 1811 when Sir Humphrey Davy first observed the crystallization of chlorine hydrates (Sloan et al. 2009; Atilhan et al. 2012). Hydrates are ice-like crystals (clathrate) formed when water and gas come into contact at elevated pressure and low temperatures (Sloan et al. 2009; Sloan and Koh 2008; Carolyn et al. 2011). About 80 mol% of gas hydrates is water and therefore many of their properties are similar to those of ice. Since this discovery, hydrate formation in hydrocarbon transportation pipelines has led the industry to inject millions of dollars to avoid pipeline blockages and other hydrate formation-related issues. To develop an operating and design philosophy to transport and/or identify the flow ability of hydrate slurries, the impact of hydrates on properties of fluid flow must be understood. If rheological parameters of the flowing fluid are not properly determined, flow modeling and design become difficult (Simon 2004; Zhang et al. 2014). Rheological characterization of hydrate slurries is critical to developing pipeline operating guidelines and

✉ Ben Bbosa
emmanuel-bbosa@utulsa.edu

[1] SPE, The University of Tulsa, Tulsa, USA

developing rheological models (Eric et al. 2013). The rheological characterization of complex fluids has been studied using flowloops (Bbosa 2015; Sinquin et al. 2004; Haghighi et al. 2007; Hald and Nuland 2007; Andersson and Gudmundsson 1999, 2000; Lv et al. 2012; Chen et al. 2014) and a high-pressure mixer-viscometer (Bbosa et al. 2017; Camargo et al. 2000; Eric et al. 2013, 2012; Ahmad et al. 2017; Patrick et al. 2008). Some of the measurements on these systems assume that the resulting slurries obey the Newtonian rheological model (Haghighi et al. 2007; Andersson and Gudmundsson 2000; Camargo et al. 2000). However, when the measured viscosity was plotted against shear rate, shear thinning behavior was observed (Bbosa 2015; Sinquin et al. 2004; Bbosa et al. 2017; Eric et al. 2012; Ahmad et al. 2017; Patrick et al. 2008). There are several challenges associated with hydrate slurry characterization. These challenges are associated with the harsh hydrate formation/stable conditions of high pressure and low temperature (Bbosa 2015; Sinquin et al. 2004; Andersson and Gudmundsson 2000; Bbosa et al. 2017; Camargo et al. 2000; Eric et al. 2013). Simple rheometers are not designed to operate at high pressure or handle solids or high molecular weight hydrocarbons such as waxes and asphaltenes that may precipitate (Bbosa 2015; Bbosa et al. 2017).

Instrumentation for rheological characterization of settling slurries such as hydrates

Several researchers have used pressure–temperature (P–T) vessels (autoclaves) to generate and characterize slurries. Because of the importance of P–T vessels in characterizing and determining of slurry rheology, modifications to improve the performance of the P–T vessels have been proposed.

McNamee and Conrad (2011) noted that the side-leg that traditional autoclaves come with had several disadvantages. Uneven distribution of additives and accumulation of condensed water in the dead-leg were pointed out as examples of the disadvantages of the side-leg. They used three sets of impeller including a cylindrical stir-bar, wedge-shaped stir-bar and an overhead stirrer. They observed a lower relative standard deviation in the measured data when using wedge-shaped stir-bar or overhead stirrer than cylindrical stir-bar. They concluded that the type of stirrer had big impact on the quality of data collected. They recommended an autoclave without a side-leg because it showed a higher reproducibility of tests.

Castell-Perez et al. (1991) proposed the use of an anchor stirrer for fluids with complex rheology. They recommended the use of mixer-viscometer when dealing with characterization of mixtures that could separate, i.e., suspensions with particles that could settle, deposit, or aggregate. La Fluente et al. (1996) studied fluids with complex rheology using helical blades impellers. They observed that impeller pitch and blade width did not affect the shear rate coefficient (the constant of proportionality between shear rate and rotational speed).

For anchor and helical blades impellers, laminar flow can still be achieved at Reynolds numbers above 100 (La Fuente et al. 1998). The laminar flow is when the Power number is inversely proportional to the Reynolds number on the Power curve. This technique can be used to identify laminar data and thus determine slurry rheology.

La Fluente et al. (1998) examined the suitability of the different impeller geometries in characterizing suspensions. They measured the torque response for helical blades agitators, cone and plate, and Couette geometries while mixing clay suspensions. They observed that the Couette and cone and plate geometries produced unstable torque responses, whereas the helical blades impeller generated a smooth torque signal. They attributed the instability in torque signal to particle–wall interaction due to poor homogenization of the suspension and less effective bulk shear. La Fluente et al. (1998) noted some additional challenges in characterizing non-homogeneous suspensions with a conventional rheometer. They noted that wall slippage and fouling of the gap might lead to erroneous results.

To develop a more effective viscometer for characterizing settling slurries such as hydrates, the viscometer should be designed with helical blades impeller and with no side-leg. A mixture viscometer was designed, built and calibrated for this study and the details are published elsewhere (Bbosa 2015; Bbosa et al. 2017).

Relating measured parameters to the rheological models

Besides equipment design, data interpretation is another challenging aspect of rheological determination and slurry characterization. For a rheometer, the flow model is mathematically well-defined, that is, the shear stresses and shear rates can directly be computed. However, for complex geometries such as the helical blades impeller, flow models are not straightforward.

The underlying principle in developing a mathematical model to interpret the measured parameter from the mixer-viscometer is to assess the system power consumption (James and Steffe 1996). Dimensionless analysis of the power consumption using the Buckingham Pi theorem has shown that the power number is a function of several other dimensionless groups. However, for laminar flow of homogenous systems, the power number is inversely proportional to the Reynolds number and the constant of proportionality is a geometric constant. This principle is straight forward for Newtonian fluids but becomes difficult for systems with complex rheology since the viscosity is a function of the shear rate.

Metzner and Otto (1957) proposed a linear relation between the shear rate and rotational speed for power law

fluids. They introduced the concept of effective viscosity and generalized Reynolds number for power law fluids. Using these concepts, they extended the power consumption technique to non-Newtonian systems. The generalized Reynolds number was calculated using the impeller diameter and the fluid effective viscosity. However, defining the impeller diameter can be challenging especially for complex geometries such as the helical blades and the anchor impeller.

Choplin and Marchal (1997) and Guillemin et al. (2008) proposed approximating the flow through the complex impeller geometry as Couette flow and applying the Couette flow analog concept. Using this concept, the measured torque and shaft speed data can be transformed into shear stress and shear rate information respectively. They observed a good agreement between the Couette analogy data and the rheometer data.

However, some challenges regarding data interpretation still remain. Johnston and Ewoldt (2013) used a double gap geometry to demonstrate the effect of surface tension. At low shear rates, torque measurements maybe erroneously high due to high surface tension. They termed this effect surface tension phenomenon. In their study, they used water and *n*-decane. These two have comparable viscosities but the latter has a lower surface tension about a third of the former. The surface tension phenomenon may be interpreted as shear thinning behavior if the measured data is not properly examined.

The above challenges were addressed while developing mathematical model to translate the measured parameters into viscosity and the details are published elsewhere (Bbosa 2015; Bbosa et al. 2017).

Hydrates slurry characterization and rheology determination

Sloan and Koh (2008) and Patrick et al. (2008) investigated the rheological behavior of hydrate slurries using a concentric cylinder rheometer. They measured the slurry viscosity and yield stress. The slurry viscosity was found to be in the range of 400–600 cp. The measured yield stress was found to be in the range of 10–70 Pa. These results could be affected by hydrate aggregation and breakup. They concluded that the Bingham model was sufficient to model the observed data (Eric et al. 2013; Patrick et al. 2008).

Camargo et al. (2000) characterized hydrate slurries using mixer-viscometer. They noted that hydrate slurries formed from Newtonian emulsions (30% watercut) showed shear thinning behavior. The apparent viscosity and shear thinning behavior increased with increasing hydrate fraction. Viscosity increased with decreasing shear rate until a certain shear rate below which viscosity does not change anymore. This viscosity behavior was attributed to formation and breakage of hydrate aggregates and became more pronounced at high watercuts (50% watercut). They concluded that 50% watercut tests had a higher solid fraction resulting in a more heterogeneous system. To improve hydrate slurry homogeneity, the use of anti-agglomerants has been proposed (Moradpour et al. 2011).

Moradpour et al. (2011) examined the use of anti-agglomerants in transporting hydrate slurries. They used 60% watercut systems to show that hydrate slurries up to 30% solid fraction could be transported without blockage. They used 600 cp mark as the transition to heterogeneous system leading to blockage. This is because the measured viscosity generally increased exponentially above 600 cp. The viscosity was estimated using a calibration curve developed with Newtonian fluids. At 60% watercut, a 1% anti-agglomerate (AA) dosage was sufficient but higher dosages were required for higher watercuts. They observed that tests without AA exhibited exponential viscosity rise at hydrate volume fraction (HVF) around 5%, whereas higher AA concentrations delay this exponential behavior to higher solid fractions, up to 30%. The effectiveness of the AA was greatly affected by oil chemistry. Tight emulsions from crude oils enhanced AA performance as opposed to loose emulsions. They concluded that water continuous emulsions could transport more hydrates compared to oil-continuous emulsions if sufficient AA concentrations were used.

A literature review of hydrate rheological characterization has revealed that there are a few studies in this area. This lack of extensive investigation into a challenge that poses significant economic risk to the oil/gas industry may be attributed to the complexity of hydrate formation conditions and agglomeration of hydrates. These hydrate formation conditions make the equipment design and rheological determination more difficult. Another problem is that hydrate density is between that of oil and water. This is a problem because the density difference is narrow and therefore correlating variations to flow properties is challenging.

In summary, several characterization techniques have been deployed to determine the rheological behavior of hydrate slurries. The use of a mixer-viscometer has been proposed for general slurry characterization studies. However, transformation of the measured data into viscosity information is not well-addressed. We have developed an in-house mixer-viscometer that addresses most of the challenges reported in literature (Bbosa 2015; Bbosa et al. 2017). There is an apparent need therefore to use the same system to generate viscosity trends and study the effects of different oils, watercuts and anti-agglomerant dosage on hydrate slurry rheology. This work aims to generate significant amount of hydrate slurry characterization data that may be used as basis for better rheometer designs, hydrate slurry flow properties modeling or integration of hydrate transportability into general multiphase modeling.

Understanding system response using cyclopentane to generate hydrates at atmospheric pressure

To have a feel of the likely response from the viscometer, a prototype benchtop arrangement was designed to study cyclopentane hydrates. Cyclopentane form structure II hydrates at atmospheric pressure at 45 F. The hydration number of cyclopentane hydrate formation is 17. This prototype setup consisted of a 2000 ml jacketed beaker, a table-top chiller, a mixer with the capability of translating current consumption into torque, and a data acquisition system. The shaft was attached to a double-helical impeller to improve load sensitivity, mixing and heat transfer. Figure 1 shows the prototype setup used for the feasibility studies with cyclopentane.

Results and discussion from the prototype tests

Cyclopentane hydrates were successfully formed at atmospheric pressure. Torque readings were recorded to capture hydrate formation and the effect of increasing hydrate volume fraction (HVF). A total of six trial runs were conducted using tap water and cyclopentane hydrates. Different watercuts were used to control the amount of hydrates formed. The effects of shaft rotational speed and hydrate volume fraction were studied. Cyclopentane hydrates are known to contain 17:1 mol ratio of water to cyclopentane (or 77% v/v water and 23% v/v cyclopentane). A theoretical solid fraction was calculated assuming 100% conversion of the limiting reactant. Hydrates were assumed to be carried by the phase that was not completely converted, that is the continuous phase. The total volume of the water and cyclopentane mixture used was maintained at 1400 ml but varied fractions of each phase. The test matrix for the trial runs is presented in Table 1. From the stoichiometric ratio of 17:1, runs 0, 1 and 2 were expected to be cyclopentane continuous, and runs 3 and 4 water continuous. Run 5 used the same composition as run 2 but with a higher shaft speed. Figure 2 shows the torque response during hydrate formation at 200 RPM. In Fig. 2, the hydrate onset occurs after about 5 min (360 s).

Figure 2 shows that during hydrate formation there were two types of torque responses—one that is exponential and the other that is gradual. The exponential torque behavior was observed with cyclopentane continuous mixtures (runs 0, 1 and 2). This exponential torque behavior collapsed afterwards. The magnitude and timing of this exponential behavior is dependent on the watercut and solid fraction. Intermediate watercut (50%) showed early exponential torque onset, but high HVF exhibited higher magnitudes. For water continuous runs, the increase in torque was mostly gradual (runs 3 and 4). Visual observations indicated that this sharp torque increase was observed when hydrates start to separate out of solution, peak occurs when most of the hydrates move to wall and torque suddenly drops when shaft starts to sweep only cyclopentane as shown in Fig. 3.

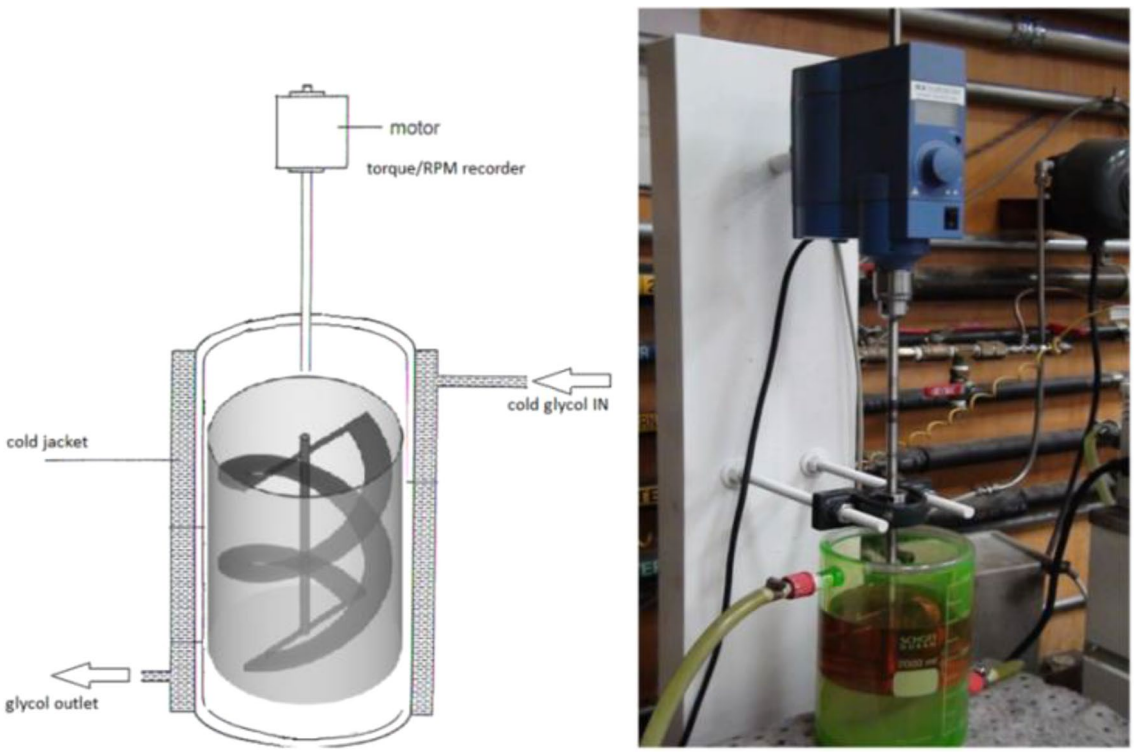

Fig. 1 Prototype setup used for the feasibility studies with cyclopentane (Bbosa 2015)

Table 1 Test matrix for the cyclopentane trial runs

Run	Water cut (%)	Water (ml)	Cyclopentane (ml)	RPM	Maximum hydrate fraction, SF (%)	Continuous phase
0	50	700	700	200	65	Cyclopentane
1	64	900	500	200	83	Cyclopentane
2	71	1000	400	200	93	Cyclopentane
3	79	1100	300	200	92	Water
4	86	1200	200	200	61	Water
5	71	1000	400	300	93	Cyclopentane

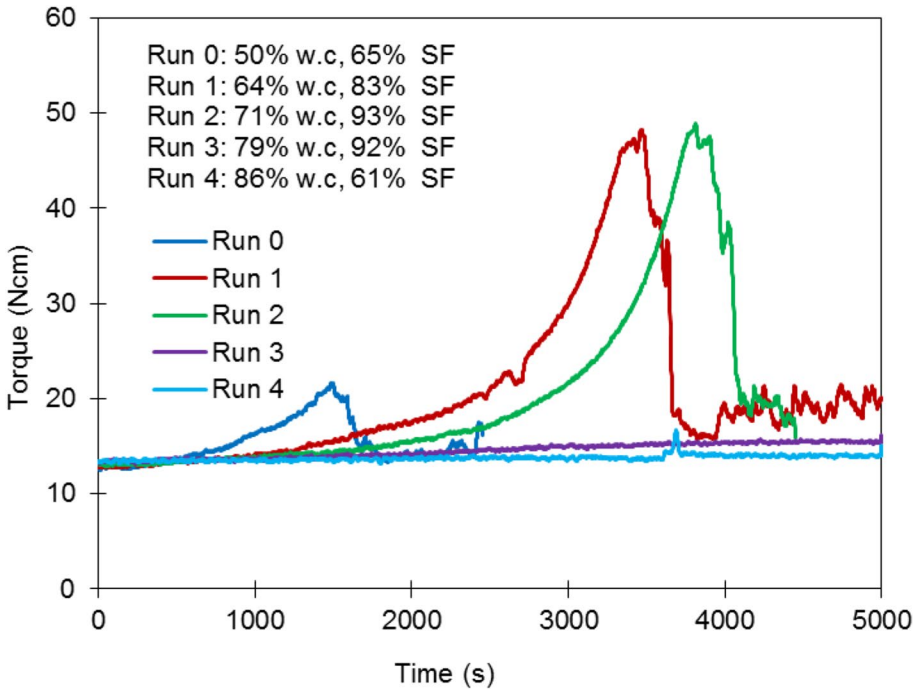

Fig. 2 Torque response during cyclopentane hydrate formation. *W.C* watercut, *SF* solid fraction

The tendency for the slurry to separate is greatly reduced by increasing shaft speed. Figure 4 shows two experiments with the same charge but conducted at different shaft speeds. It was noted that the experiment which ran at a higher speed (300 rpm) showed gradual torque increase, whereas the experiment that ran at a lower speed (200 rpm) exhibited separation behavior and thus an increase in exponential torque. Forming hydrates at low mixer speeds results in heterogeneous slurry and an exponential increase in torque. At some point after heterogeneous slurry is formed, deposition on the wall occurs leaving less solids in the flow stream and, thus, resulting in rapid torque decay. At higher shaft speed, this phenomenon was not observed and the mixture remained homogeneous.

Torque behavior during shaft speed ramping was also studied. This is necessary and required to collect shear stress as a function of shear rate. Shaft speed ramps performed on runs 2 and 5 are summarized in Fig. 5. Torque reading for Run 2 collapsed when shaft speed decreased below 400 RPM. On the other hand, torque decreased proportionally with shaft speed for Run 5. This suggests that there is a minimum shaft speed required to maintain hydrates suspended.

Lessons learned from the prototype tests

1. *Scalability of results* Previous studies at The University of Tulsa Hydrates Flow performance Project (TUHFP) showed pressure drop trends similar to torque behavior presented in Fig. 4 (Deepak and Montereiro 2011; Emmanuel; Dellecase et al. 2008; Douglas and Estanga 2007; Oris and Hernandez 2006). These studies, conducted on flowloop, showed that experiments conducted at low shear rates exhibited exponential pressure buildup whereas tests performed at high shear rates showed gradual pressure drop increase with increase in HVF. Other factors also contributed to exponential pressure drop increase including high watercuts and high hydrate

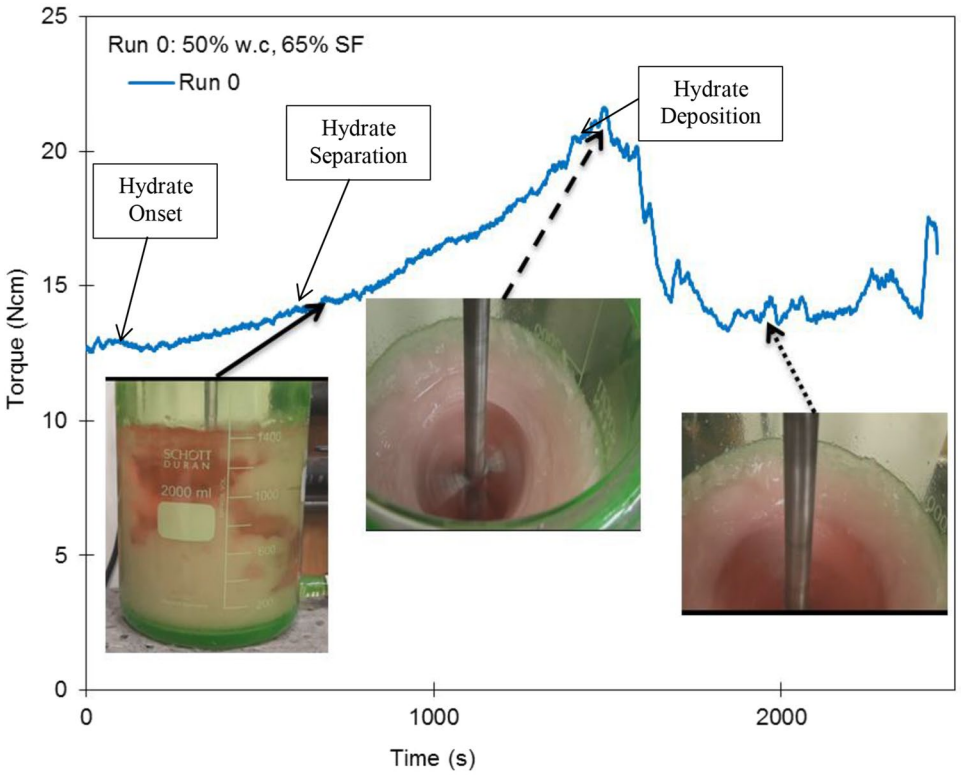

Fig. 3 Visual observation of cyclopentane hydrate mixture with time. *W.C* watercut, *SF* solid fraction

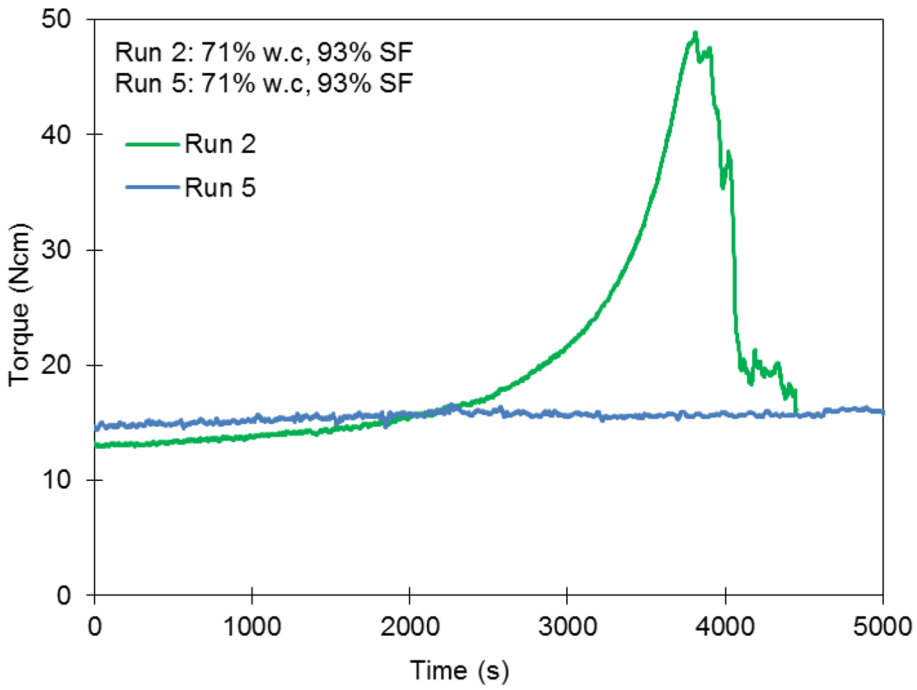

Fig. 4 Effect of mixer speed on hydrate slurry behavior. *W.C* watercut, *SF* solid fraction

volume fraction (Deepak and Montereiro 2011; Emmanuel; Dellecase et al. 2008). Well-dispersed systems exhibited a gradual increase in the pressure drop. This is important because flow loop tests which require large quantities can now be planned by scaling up benchtop result by directly correlating pressure drop to torque. Cyclopentane tests gave useful insights on mixer response to hydrate formation and how to relate this to flow loop observations.

2. *The role of AA* Without AA hydrates agglomeration result in early onset of exponential torque (or pressure drop) increase and early deviation from Newto-

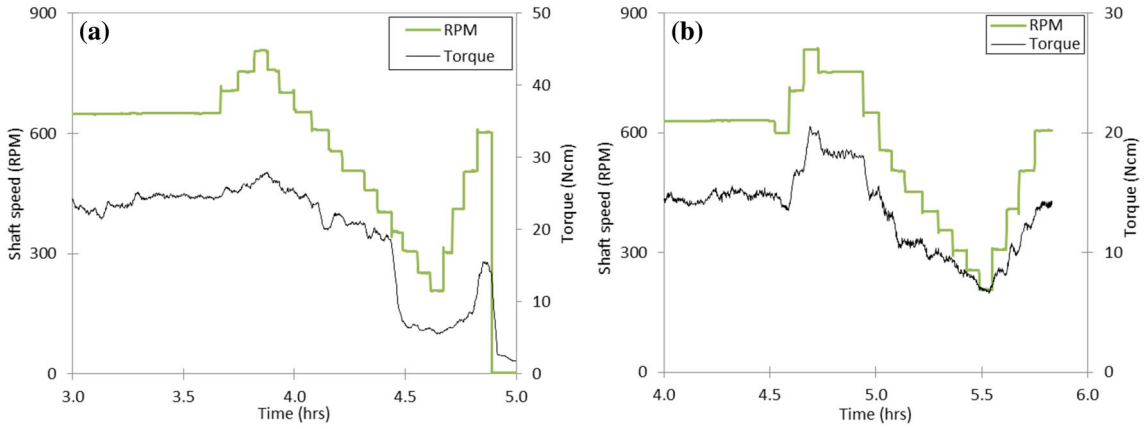

Fig. 5 Torque response during shaft speed ramps, **a** run 2, and **b** run 5

nian rheology. This may be attributed to onset of solid concentration gradient as demonstrated from the prototype setup. Use of AA minimizes agglomeration and promotes dispersed slurries. dispersed (homogeneous) slurries exhibit Newtonian rheology. Newtonian slurries display gradual increase in viscosity with increase in HVF. However, at high HVF, AAs fail and agglomeration occurs. Slurries that experience severe agglomeration flow with a radial solid concentration gradient and exhibit shear thinning rheology. This suggests that shear thinning (or non-Newtonian) behavior of hydrate slurries is associated with particle interaction, agglomeration and solid concentration gradient.

3. *Heterogenization: detection and avoidance* Cyclopentane tests showed that the generated slurries can be dispersed or segregated slurries. The type of slurry formed may depend on the fluid mixture charged to the system, operating conditions and additives used. Figure 6 shows a hypothetical torque response during hydrate formation. Heterogeneous slurries may result from severe agglomeration or settling of hydrate particles. Figure 6 also shows the effect of some unit operations and experimental conditions on the resulting viscosity and slurry type. On the other hand, torque signature may give indications whether the slurry is dispersed/ homogenous (no concentration gradient) or heterogeneous (with concentration gradient). This is important because viscosity can only be established with homogeneous systems. During shaft speed ramping, if solids agglomerate towards the mixing blade, torque is expected to rise. However, if the agglomerating solids

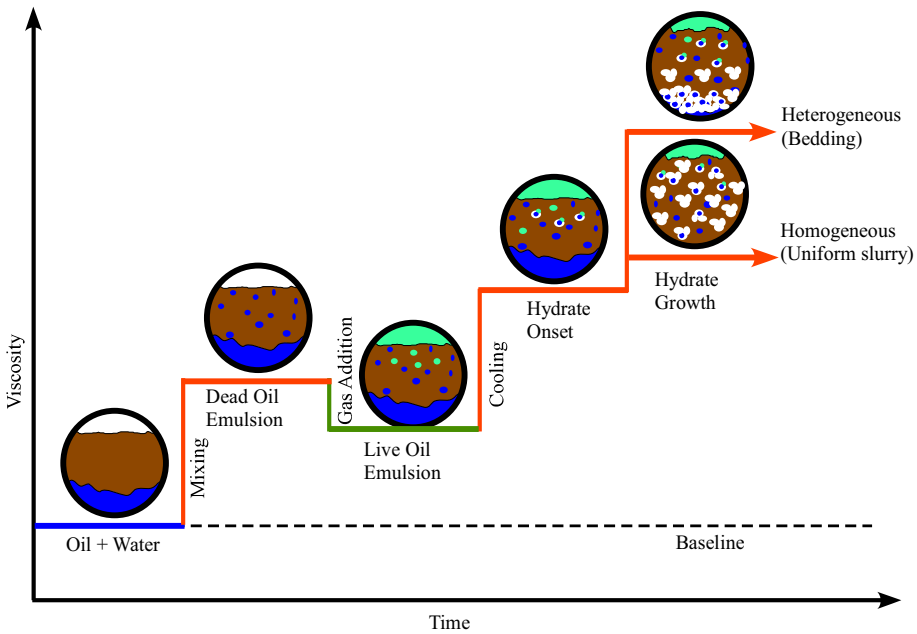

Fig. 6 Hypothetical torque response during hydrate formation

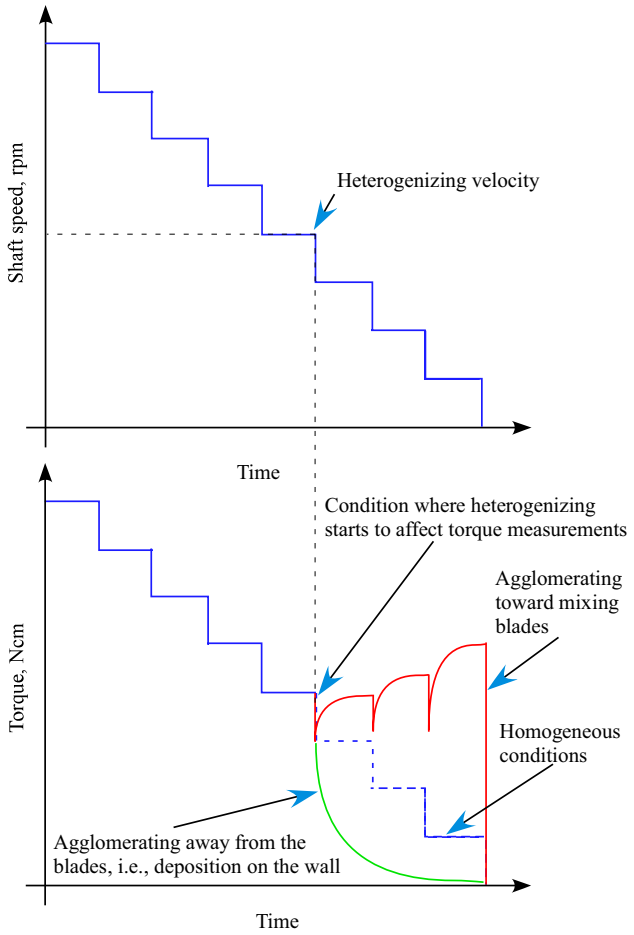

Fig. 7 Hypothetical torque response during shaft speed ramp down

move away from the blades, i.e., toward the wall, torque measurements decrease. Figure 7 shows a hypothetical toque response during shaft speed ramp down.

Experimental facility and procedures

Facility

The test facility consisted of mixer-viscometer, a gas addition system, a cooling system, a liquid charge system, cleaning solvent charge systems, and a data acquisition system. The gas charging system consisted of a pressurized gas bottle (usually 1800 psi), a pressure regulator, gas cooling bath and a mass flow meter. Operating pressure was preset using the pressure regulator. The gas through the preset pressure regulator was routed through an ice bath to cool it before it was metered. A Porter series 200 mass flowmeter was used to meter the flow rate and total volume of gas added to the vessel. The liquid charging system consisted of a simple funnel through which liquids were added to the vessel. The liquid charge could also be done using the cleaning system especially if it was desired to add liquid when the vessel was already pressurized. The cleaning and venting system consisted of a pump, bottom valve, drain trough and a vent. The pump could be used to draw liquid from the selected tank and send it to the vessel. The liquid could be a reactant or just cleaning solvent. The bottom valve was used to let in liquids into the vessel or drain from it. The drain trough was used to collect wastes after the experiments. The cooling system consisted of a chiller, the gas temperature control bath and a cooling jacket. The chiller was used to heat, cool or maintain temperature of the vessel contents. The gas temperature bath was intended to pre-cool the gas on hot days when the ambient temperatures were extremely high. The cooling jacket was the main heat exchange point between the chiller and the vessel contents. The shaft magnetic coupling was cooled to prevent heating due to friction. The mixing system consisted of a motor drive, torque sensor, and impeller. The vessel was 3.25″ internal diameter, 10″ height and rated for a maximum working pressure of 3000 psi. It was equipped with gas inlet and outlet valves, a sampling/drain valve at the bottom, pressure gage, safety/relief valve, and internal thermocouple. A ¼ HP variable speed motor was used to rotate the mixing shaft from 0 to 1900 rpm. A rotary shaft non-contact torque sensor model 01424 was used to measure torque directly from the shaft. A helical-blade impeller with two ¼ pitch blades was used for mixing vessel contents. The helical blades impeller was found to be more sensitive to viscosity change and hydrate formation during the trial tests. It also reduces the formation of a vortex during mixing. The process control and data acquisition system was developed using Factory Talk integrated suite software from Rockwell Automation. The recorded variables were shaft rotational speed, torque on shaft, chiller temperature, gas bath temperature, vessel temperature, vessel pressure, gas injection rate and totalized gas volume. A detailed description of the design, mathematical models, and calibration for this mixer-viscometer is published elsewhere (Bbosa 2015; Bbosa et al. 2017) Fig. 8 shows the Piping and Instrumentation Diagram (P&ID) for the setup. Figure 9 shows the schematic of the in-house mixer-viscometer used in characterization of hydrate slurries. Figure 10 shows the small-scale facility setup.

Experimental procedure

At the start of the test, the vessel was charged with known volumes of oil and brine. The liquids were then mixed at 650 rpm well above the speed at which separation was observed during cyclopentane tests. Gas was then added to maintain pressure at 1100 psi while maintaining temperature at 70 °F. Mixing was continued for 10–30 min before cooling was started. At hydrate formation onset the gas counter was reset and desired amount of gas was added to generated amount of hydrates.

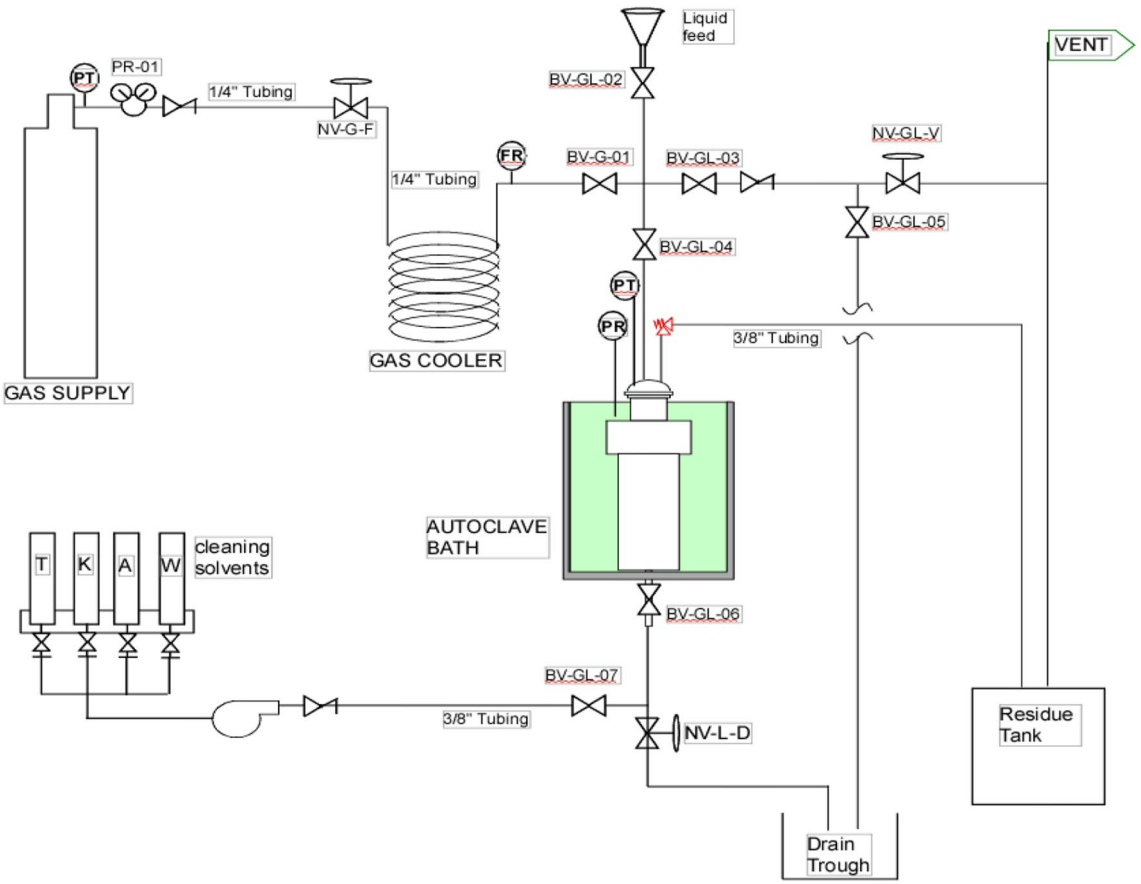

Fig. 8 P&ID for the mixer-viscometer setup

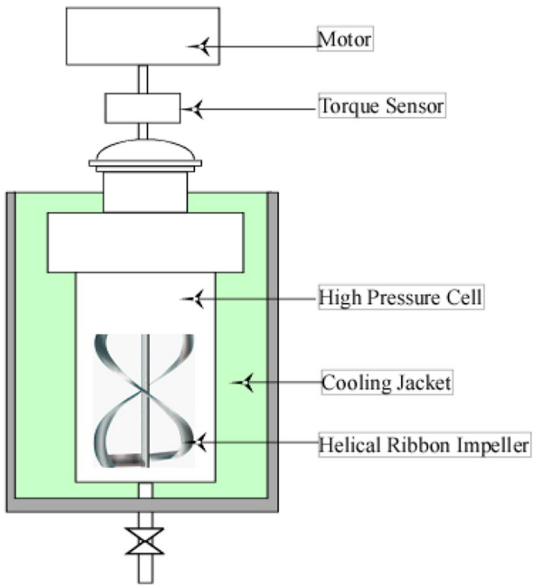

Fig. 9 Schematic of the in-house mixer-viscometer used in characterization of hydrate slurries

Gas supply was then cut off and the system was allowed to stabilize to a new pressure. Shaft speed ramping was then performed to establish the rheology of the flowing hydrate slurry. Shaft speed ramping involved increasing the speed from 600 to 800 rpm, decreasing the speed from 800 to 200 rpm, and then back to 600 rpm. This ramp ensured laminar regime at low shaft speeds and also checking separation behavior of the slurry. Ramping back to 600 rpm compares the slurry behavior before and after the ramp. Hysteresis provides useful information about yield stress behavior of the slurry.

Test fluids

The oils used were kerosene, PA-3 and Crystal plus 70FG. Kerosene was selected to represent low viscosity oils and Crystal plus 70 FG to represent high viscosity oils. PA-3 is a well-characterized GOM analog with intermediate viscosity. The viscosity–temperature plot for the oils used is shown in Fig. 11. The brine used was 3.5% wt/wt NaCl. To generate homogeneous slurry, an anti-agglomerant "A" was used at 3%v/v dosage with respect to brine for all watercuts. For all tests, Tulsa city gas with a typical molar composition of about 95% methane, 2.5% ethane and 2.5% propane was used

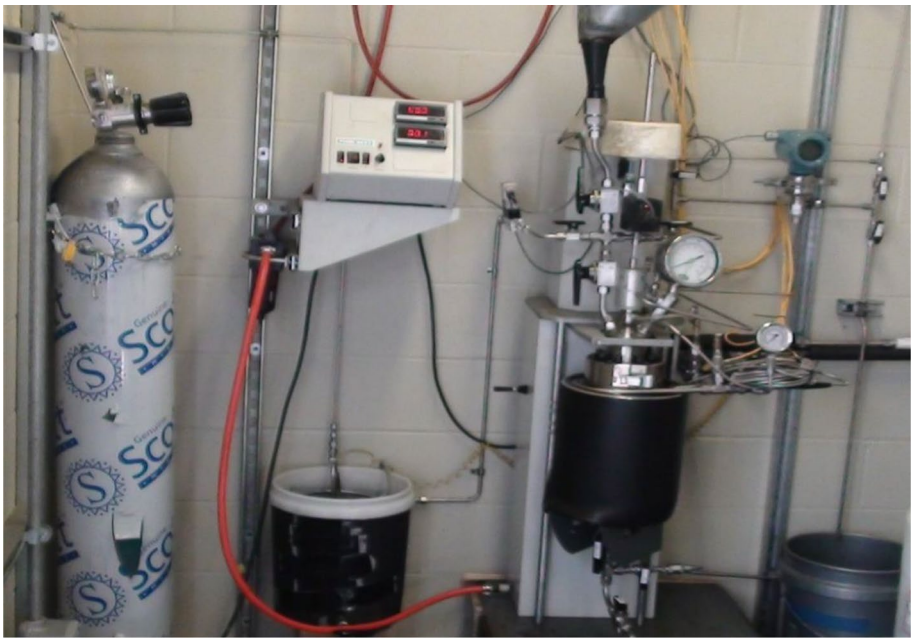

Fig. 10 Small-scale facility

as the hydrate former. The amount of hydrates formed was estimated from gas material balance and system PVT measurements. Tests were performed at 30, 50 and 70% watercut. At the same watercut, different amounts of gas were injected to generated slurries with different hydrate volume fractions (HVFs).

Results and discussion

Characterization experiments were conducted to generate both homogeneous and heterogeneous slurries. Experimental conditions that led to heterogeneous slurries were high watercuts, low shaft speed, high HVF and low or no additives. On the other hand, homogeneous slurries were generated under conditions of high shaft speeds and presence of additives. For ease of classification, all tests with no anti-agglomerant were placed under heterogeneous slurry tests and all anti-agglomerants under homogeneous slurry tests.

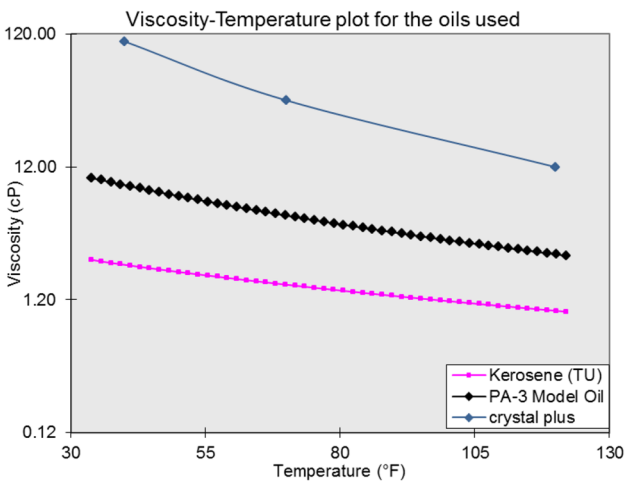

Fig. 11 Viscosity–temperature plot for the oils used to make hydrates slurries

Homogeneous slurry

Kerosene results

Figure 12 shows the raw data collected from 30% watercut test. The plot can be divided into four zones. The first zone (Zone I) is pre-hydrate formation and mainly involves cooldown and pressure maintenance. The second zone (Zone II) is the hydrate formation and gas addition zone which starts from hydrate formation onset (HFO) and ends when gas is cutoff. The third zone (Zone III) is the stabilization zone during which no gas is added but hydrate formation continues until pressure stabilizes or decreases by less than 25 psi in an hour. The last zone (Zone IV) is speed ramping zone during which rheological data is collected. Data on this plot starts 0.25 h before hydrate formation onset. Data recorded includes pressure (psia), shaft speed (rpm), gas flow rates (ml/min), vessel temperature (°F) and shaft torque (N cm). Data collected from Zone I may be used to correlate the carrier fluid viscosity to parameters such as watercut, gas oil ratio (GOR), temperature and oil API. This work is ongoing at The University of Tulsa. HFO marks the start Zone II. HFO was observed at 42 °F and was accompanied by pressure decrease, temperature increase due to exothermic nature of hydrate formation, and torque increase capturing

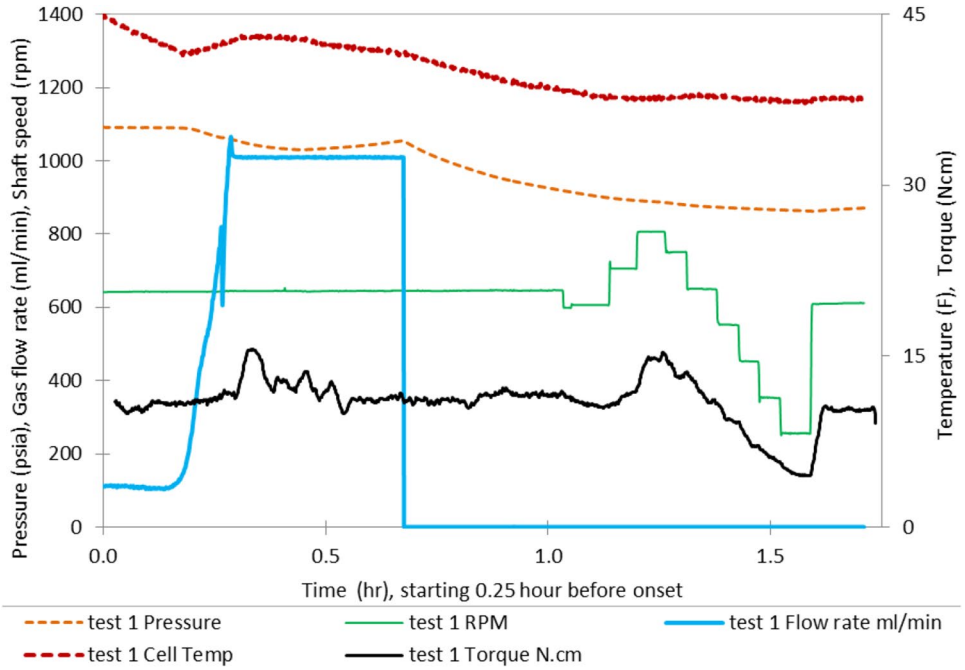

Fig. 12 Typical temperature, pressure, gas, and torque profiles of a kerosene–water hydrate transporting system in a the mixer-viscometer device. This test contains 30% watercut. Initial pressure was 1100 psi at 70 °F. The jacket temperature was decreased from 70 °F and maintained at 40 °F

changes in viscosity. HFO leads to gas consumption from the flow mixtures which results in "dead" oil–water mixture momentarily triggering spikes in torque. This is a transient mass transfer phenomenon and should not be interpreted as viscosity change. The gas flow meter was set to provide gas to the system at a rate up to 1000 ml/min to maintain pressure at 1100 psi. So during cooling gas was added at a low flow rates to compensate for volume shrinkage due to temperature decrease. However, at HFO gas flow rate jumped to the maximum allowable flow rate of 1000 ml/min. This meant that if the gas consumption due hydrate formation was higher that gas flow rate then system pressure would decrease. And when hydrate formation slowed down, system pressure would be maintained at 1100 psi. Data collected in Zone II is useful when modeling the transient behavior or system response during hydrate formation. During zone III, the vessel temperature approached the jacket temperature, vessel pressure decreased to a new value close to 850 psi, and torque stabilized. During this zone, hydrate formation continues. Generally, torque increases due to formation of more hydrates and gas consumption both of which lead to increase in slurry viscosity. Shaft speed ramps are performed in Zone IV. It should be noted that torque responded proportionally to shaft speed changes confirming that the slurry generated in this test were mostly dispersed. Also, the torque observed at 600 rpm at the end of Zone IV was close to the value observed at the start of the zone suggesting little to no yield stress.

For characterization purposes, average torque values at different shaft speeds were collected. Figure 13 shows the average torque values plotted against shaft speed. For any given watercut, torques (and viscosity) increase with hydrate volume fraction (HVF). The measured torque was then converted to viscosity (details are published elsewhere Bbosa 2015; Bbosa et al. 2017). Figure 14 shows the calculated viscosities for the kerosene tests. It can observed from the figure that intermediate watercut (50%) hydrate slurries exhibited shear thinning behavior that increased with increasing HVF (Eric et al. 2012; Ahmad et al. 2017). On the other hand, low watercuts (30%WC) and high watercut (70%WC) exhibit Newtonian rheology at low HVF but develop shear thinning behavior as HVF increases. There are three main factors that affect hydrate slurry viscosity. The first factor is the HVF. Several studies have observed that viscosity increases as the system transforms from gas–liquid to gas–liquid–solid (Ahmad et al. 2017). However, it should also be noted that the increase is proportional to HVF if the hydrates are fully dispersed. The second factor is gas mass transfer. During hydrate formation, gas is consumed from the liquid mixture and if gas movement from the gas bulk to the hydrate forming sites is not the same as the gas consumption then higher viscosities readings are observed. This transient viscosity is clearly observed but there is a lack of physics to properly model it. The last factor is the composition of the hydrate carrier fluid. Similarly this is a challenging topic. Several researchers have addressed a few of the variables related to composition of the hydrate carrier fluid (Ahmad et al. 2017). Some of the parameters that have been studied include pressure, temperature, watercut, oil viscosity, brine salinity, etc., but not in a single study which makes it difficult to draw conclusions. The data set provided in this study is aimed at providing insights regarding some of these parameters but most importantly to show that these studies can be done using a simple in-house device.

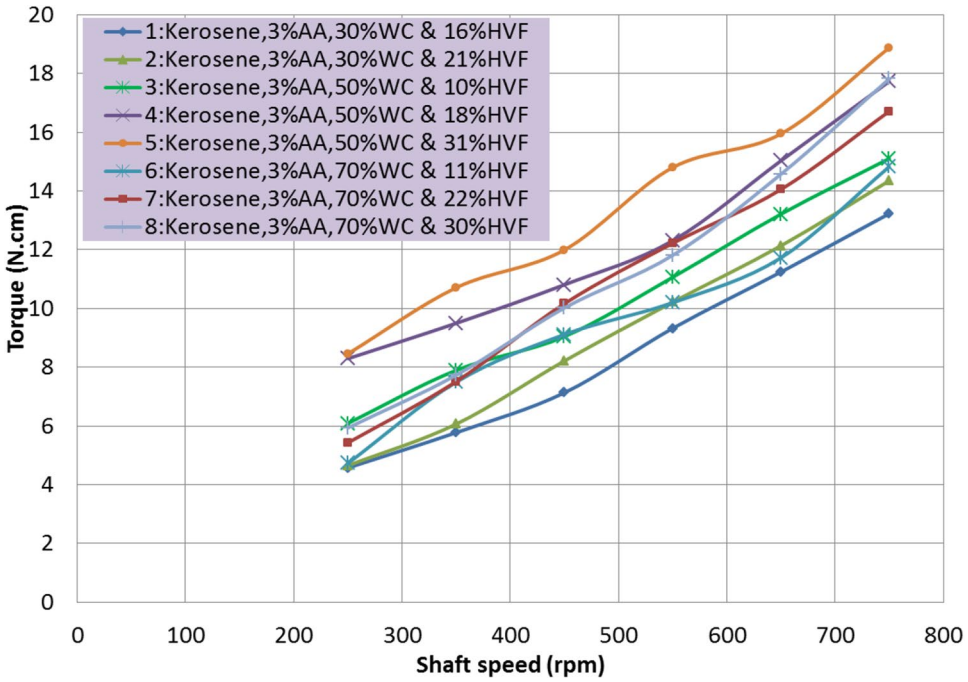

Fig. 13 Average torque values collected from Zone IV for kerosene tests. *AA* anti-agglomerant, *WC* watercut, *HVF* hydrate volume fraction

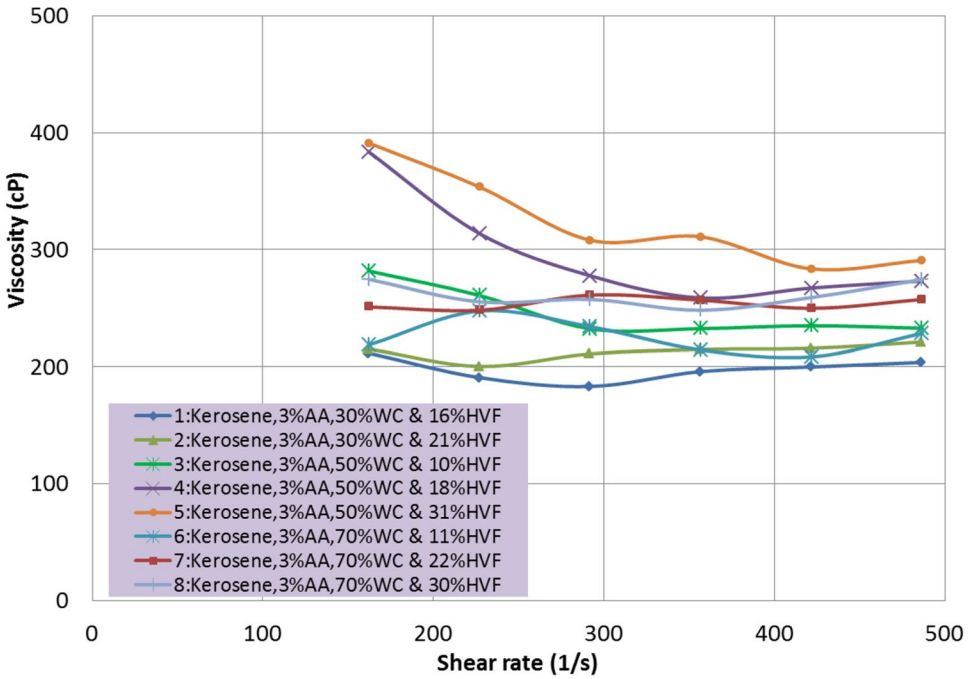

Fig. 14 In situ viscosity of hydrate slurries formed from kerosene–water systems. *AA* anti-agglomerant, *WC* watercut, *HVF* hydrate volume fraction

PA-3 results

Data collected from the PA-3 tests was treated in the same way as kerosene data. Figure 15 shows the average torque values collected from Zone IV. At HVF of 28% and above, torque values collapsed when the shaft speed decreased below 450 RPM. As discussed under cyclopentane results, this indicates separation or onset of heterogeneous mixture. Factors that promote heterogeneous mixtures were discussed earlier including high HVF. However, use of AA is expected to help. Observation of this separation indicates that AA may be limited on how many hydrates they can disperse. Data exhibiting heterogeneous behavior was eliminated while computing viscosity. Figure 16 shows the calculated viscosities for the PA-3 tests. Intermediate watercuts (50%) hydrate slurries generally exhibited high viscosity and significant shear thinning behavior that increased with increasing HVF (Eric et al. 2012; Ahmad et al. 2017), while low

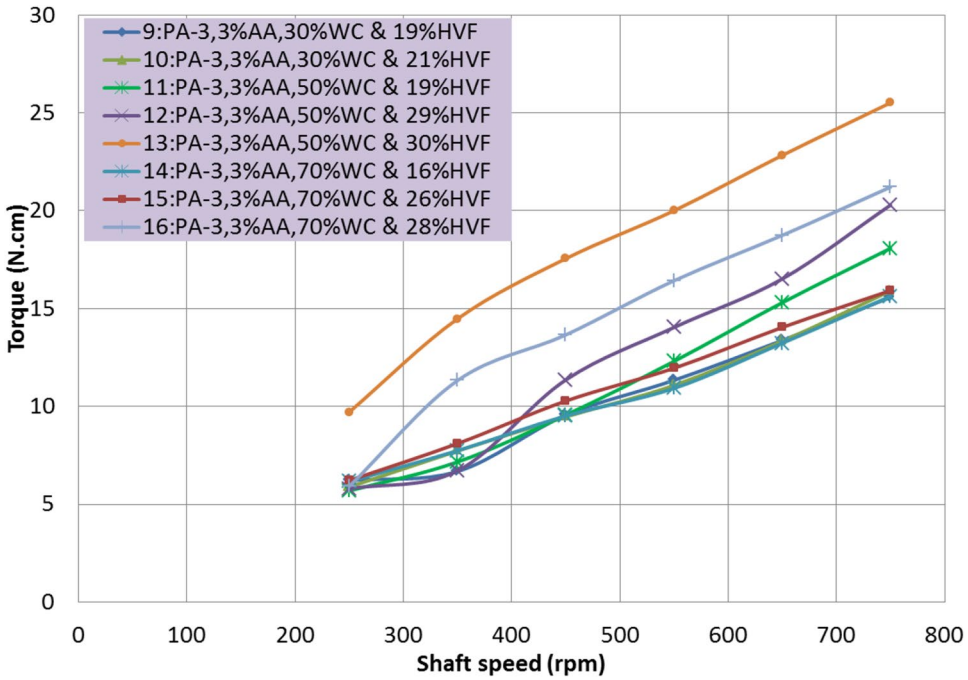

Fig. 15 Average torque values collected from Zone IV for kerosene tests. *AA* anti-agglomerant, *WC* watercut, *HVF* hydrate volume fraction

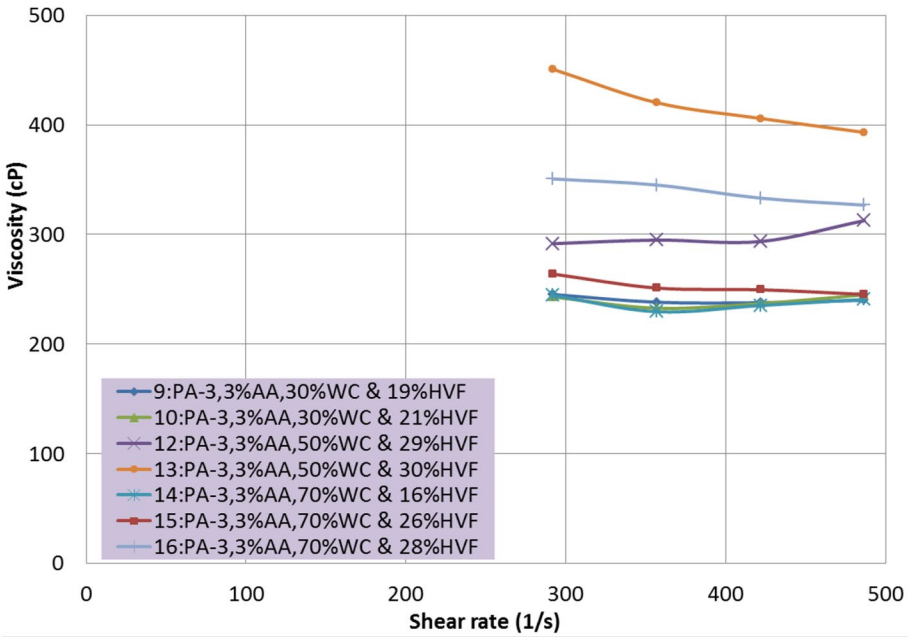

Fig. 16 In situ viscosity of hydrate slurries formed from PA-3-water systems. *AA* anti-agglomerant, *WC* watercut, *HVF* hydrate volume fraction

watercuts (30%WC) and high watercuts (70%WC) exhibited weak shear thinning behavior that increased with HVF. The inability of PA-3 to transport hydrates at low shear rates suggests that hydrate transportability is a function of oil properties.

Crystal Plus 70FG (CP70FG) results

Lastly, data collected from the CP70FG tests was treated in the same way as kerosene data. Figure 17 shows the average torque values collected from Zone IV. For CP70FG, heterogeneous behavior was observed at HVF of 23% and above for the 50% watercut tests and above 30% for the 70% watercut tests. It should be noted that all the oils used in this study do not form emulsions with water under the test conditions examined. Also, the AA used was recommended for the three oils at an effective dosage of 3%. However, results suggest that transportability fails at high HVF. Onset of heterogeneity occurs at different shaft speeds for different oils, watercut or

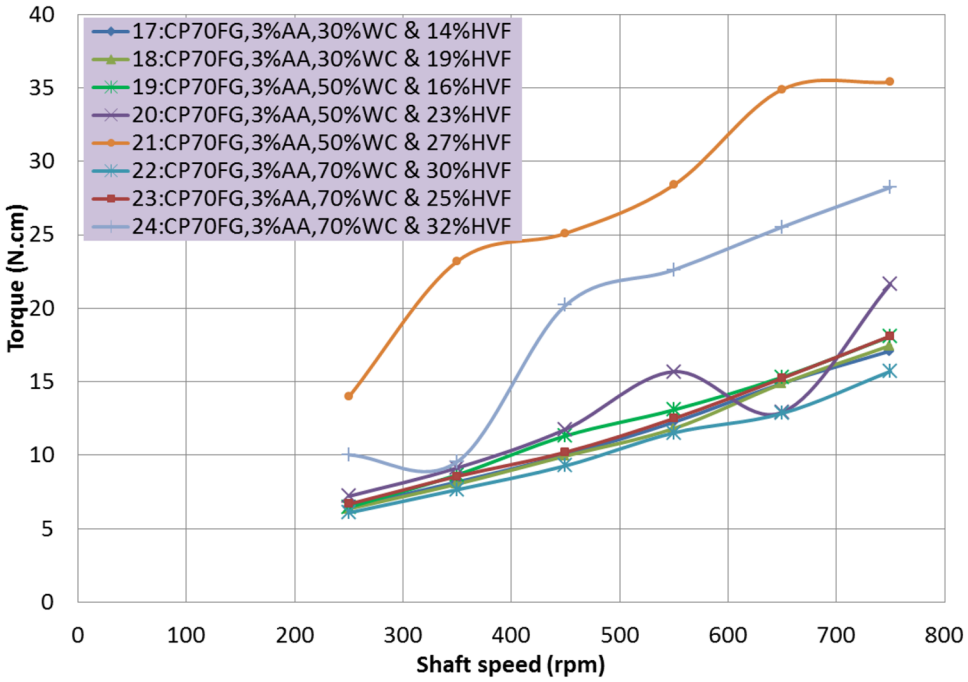

Fig. 17 Average torque values collected from Zone IV for Crystal Plus 70FG tests. *AA* anti-agglomerant, *WC* watercut, *CP70FG* Crystal Plus 70FG, *HVF* hydrate volume fraction

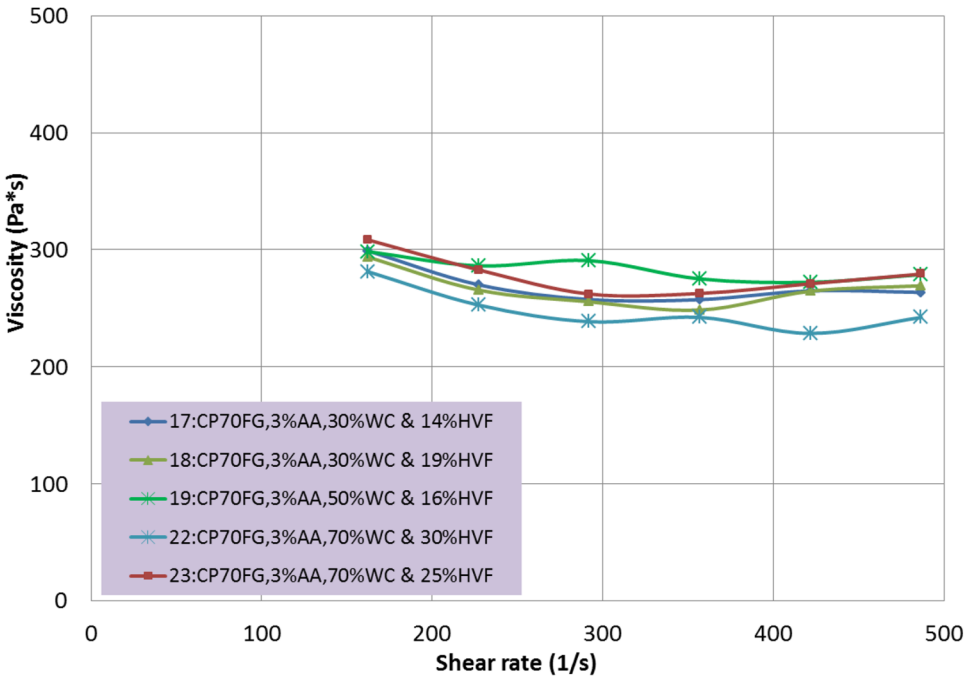

Fig. 18 In situ viscosity of hydrate slurries formed from PA-3-water systems. *AA* anti-agglomerant, *WC* watercut, *HVF* hydrate volume fraction

HVF. Data points exhibiting heterogeneous behavior were eliminated while computing viscosity. Figure 18 shows the calculated viscosities for the CP70FG tests. Intermediate watercuts posed the greatest hydrate transport risk for all oils. CP70FG hydrate slurries generally exhibited shear thinning behavior that gradually increased with HVF.

Heterogeneous slurry

Next, three tests were conducted at 70% watercut without AA, one for each oil. All tests performed without AA showed solid separation at some shaft speed (Fig. 19). The behavior observed from these tests suggests strong solid concentration gradient and separation and thus viscosity was not computed. This behavior confirms that hydrate transport without additives may lead to pipeline plugging.

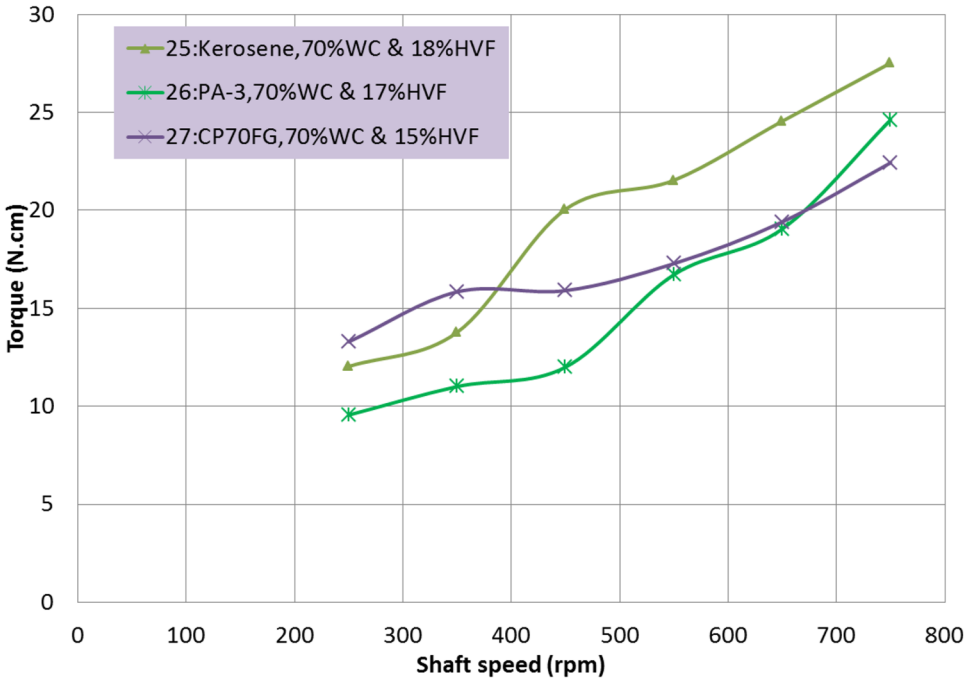

Fig. 19 Average torque values collected from Zone IV for the non-AA tests. *AA* anti-agglomerant, *WC* watercut, *CP70FG* Crystal Plus 70FG, *HVF* hydrate volume fraction

Conclusion

In this work, viscosity measurements of hydrate slurries at various watercuts, different oils and different solid fractions were performed using an in-house mixer-viscometer. The system viscosity increased during cooling. Slurry viscosity significantly increased during hydrate formation due to gas mass transfer. Shear rate changes during Zone IV provided information regarding hydrates distribution in the carrier phase.

Cyclopentane studies helped provide insights into torque response during solid separation. Torque signature during solid separation was used to distinguish between particle–wall interaction vs. solid settling.

Intermediate watercuts posed the greatest plugging risk for all the oils tested. This was attributed to phase separation which is prevalent in low viscosity oils. The oils used in this work did not form emulsions under the test conditions examined. The amount of transportable hydrates increased with oil viscosity. Generally hydrate slurries generated exhibited shear thinning behavior that increased with increasing hydrate volume fraction. However, the overall rheology of these slurries is a complex function of the oil used, watercut, gas added to the system and hydrate solid fraction. Lowering shear rates for high HVF systems resulted in separation.

In general, results in this work suggest that hydrate transportation may be possible with minimum risk if the right anti-agglomerant is used and high enough shear is applied. On the other hand, if no anti-agglomerant is used severe aggregation may result in flow line plugging.

Hydrate slurries generated without anti-agglomerant showed high shear thinning behavior and higher viscosities compared to systems with AAs. Also, shear thinning behavior increased with increasing hydrate volume fraction. Without AA hydrates agglomeration result in early onset of exponential viscosity increase and early deviation from Newtonian rheology. Use of AAs minimize agglomeration and dispersed slurries exhibit Newtonian rheology. Newtonian slurries display gradual increase in viscosity with increase in HVF. However, at high HVF AAs fail and agglomeration occurs. Slurries that experience severe agglomeration flow with a radial solid concentration gradient exhibit shear thinning rheology. This suggests that shear thinning (or non-Newtonian) behavior of hydrate slurries is associated with particle interaction, agglomeration and solid concentration gradient. When high viscosity oils were used, the resulting slurries exhibited less shear thinning effects and less viscosity increase with increasing hydrate volume fraction. This suggests that for the same AA dosage, AA performance is enhanced by high oil viscosity.

Acknowledgements We acknowledge the support accorded by The University of Tulsa Hydrate Flow Performance Project JIP member companies.

References

Ahmad AA, Majid DT, Wu, Koh CA (2017) New in situ measurements of the viscosity of gas clathrate hydrate slurries formed from model water-in-oil emulsions. Langmuir 33:11436–11445

Andersson V, Gudmundsson JS (1999) Flow experiment on concentrated hydrate slurries. SPE 56567, SPE Annual Technical Conference and Exhibition, Houston, Texas

Andersson V, Gudmundsson JS (2000) Flow properties of hydrate-in-water slurries. Ann NY Acad Sci 912:322–329

Atilhan M. Aparicio S, Benyahia F, Deniz E (2012) Advances in natural gas technology. Intech Publisher, London

Bbosa B (2015) Mechanistic modeling and experimental investigation of hydrate transportability in horizontal pipelines. PhD dissertation, University of Tulsa

Bbosa B, DelleCase E, Volk M, Ozbayoglu E (2017) Development of a mixer-viscometer for studying rheological behavior of settling and non-settling slurries. J Pet Explor Prod Technol 7(2):511–520

Camargo R, Palermo T, Sinquin A, Glenat P (2000) Rheological characterization of hydrates suspension in oil dominated systems. Ann N Y Acad Sci 912:906–916

Carolyn A, Koh E, Dendy Sloan AK, Sum, Wu DT (2011) Fundamentals and applications of gas hydrates. Annu Rev Chem Biomol Eng 2:237–257

Castell-Perez ME, Steffe JF, Rosana G (1991) Simple determination of power law flow curves using a paddle type mixer viscometer. J Texture Stud 22:303–316

Choplin L, Marchal P (1997) Mixer-type rheometry for food products. In: First international symposium on food rheology and structure. Zurich Switzerland, pp 40–44

Deepak S, Montereiro (2011) Hydrate ttransportability studies in hydrocarbon systems. Master thesis

Dellecase E, Geraci G, Barrios L, Estanga D, Dominguess R, Volk M (2008) Hydrate plugging or slurry flow: effect of key variables. In: Proceedings of the 6th international conference on gas hydrates (ICGH 2008), Canada

Douglas A, Estanga (2007) Plugging tendencies of hydrate forming systems during restart operations. Master thesis, University of Tulsa

Eric B, Webb PJ, Rensing CA, Koh E, Dendy Sloan AK, Sum, Liberatore MW (2012) High-pressure rheology of hydrate slurries formed water-in-oil emulsions. Energy Fuels 26:3504–3509

Eric B, Webb CA, Koh, Liberatore MW (2013) Rheological properties of methane hydrate slurries formed from AOT + water + oil microemulsions. Langmuir 29:10997–11004

Guillemin JP, Menard Y, Brunet L, Bonnefoy O, Thomas G (2008) Development of a new mixing rheometer for studying rheological behavior of concentrated energetic suspensions. J Non Newton Fluid Mech 151:136–144

Haghighi H, Azarinezhad R, Chapoy A, Anderson R, Tohidi B (2007) Hydraflow: avoiding gas hydrate problems. SPE 107335, EUROPEC/EAGE Conference and Exhibition, London

Hald K, Nuland S (2007) Hydrate slurry rheology in the petroleum industry. Annu Trans Nordic Rheol Soc 15

James F, Steffe (1996) Rheological methods in food engineering, 2nd edn. Freeman press, East Lansing

Johnston MT, Ewoldt RH (2013) Precision rheometry: surface tension effects on low-torque measurements in rotational rheometers. J Rheology 57:1515

La Fuente EB, Choplin L, Tanguy PA (1996) Mixing with helical ribbon impellers: effect of highly shear thinning behavior and impeller geometry. IChemE 75(1):45–52

La Fuente EB, Nava JA, Lopez LM, Medina L, Ascanio G, Tanguy PA (1998) Process viscometry of complex fluids and suspensions with helical ribbon agitators. Can J Chem Eng 76:689–695

Lv XF, Gong J, Li WQ, Shi BH, Yu D, Wu HH (2012) Experimental study of natural gas hydrates slurry flow. SPE 158597, SPE Annual Technical Conference and Exhibition, San Antonio, Texas, USA

McNamee K, Conrad P (2011) The effect of autoclave design and test protocol on hydrate test results. In: Proceedings of the 7th international conference on gas hydrates (ICGH 2011), Edinburgh, Scotland, United Kingdom, July 17–21, 2011

Metzner AB, Otto RE (1957) Agitation of non-Newtonian fluids. AIChE J 3(1):3–10

Moradpour H, Chapoy A, Tohidi B (2011) Controlling hydrate slurry transportability by optimizing anti-agglomerant usage in high water cut systems. OTC 22485, Offshore Technology Conference, Rio de Janeiro, Brazil

Oris C, Hernandez (2006) Investigation of hydrate slurry flow in horizontal pipelines. PhD dissertation, University of Tulsa

Rensing PJ, Liberatore MW, Koh CA, Sloan ED (2008) Rheological investigation of hydrate slurries. In: Proceedings 6th international conference on gas hydrates (ICGH 2008), Vancouver, British Columbia, Canada, July 6–10, 2008

Simon K (2004) The role of different rheological models in accuracy of pressure loss prediction. Rudarsko-geolosko-naftni zbomik 16:85–89

Sinquin A, Palermo T, Peysson Y (2004) Rheological and flow properties of gas hydrate suspensions. Oil Gas Sci Technol Rev IFP 59:41–57

Sloan ED Jr, Koh CA (2008) Clathrate hydrates of natural gases, vol 119, 3rd edn. Chemical Industries, CRC Press, Boca Raton

Sloan ED, Koh CA, Sum AK, Ballard AL, Shoup GJ, McMullen N, Creek JL, Palermo T (2009) Hydrates: state of the art inside and outside flowlines. 118534-JPT SPE Journal Paper, 2009

Yan K-L, Sun C-Y, Chen J, Chen L-T, Shen D-J, Liu B, Jia M-L, Niu M, Lv Y-N, Li N, Song Z-Y, Niu S-S, Chen G-J (2014) Flow characteristics and rheological properties of natural gas hydrate slurry in presence of anti-agglomerant in a flow loop apparatus. J Chem Eng Sci 106:99–108

Zhang Q, Wang Z, Wang X, Yang J (2014) A new comprehensive model for predicting the pressure drop of flow in the horizontal wellbore. ASME J Energy Resour Technol 136:042903